catalysts

MDPI

Article

# Solid-State $NaBH_4$ Composites as Hydrogen Generation Material: Effect of Thermal Treatment of a Catalyst Precursor on the Hydrogen Generation Rate

**Olga V. Netskina *, Alena A. Pochtar, Oxana V. Komova and Valentina I. Simagina**

Boreskov Institute of Catalysis SB RAS (BIC SB RAS), 630090 Novosibirsk, Russia; po4tar@catalysis.ru (A.A.P.); komova@catalysis.ru (O.V.K.); simagina@catalysis.ru (V.I.S.)

* Correspondence: netskina@catalysis.ru; Tel.: +7-383-330-74-58

Received: 23 January 2020; Accepted: 6 February 2020; Published: 7 February 2020


**Abstract:** Solid-state composites based on sodium borohydride ($NaBH_4$) were studied for applications as hydrogen generation materials. Hydrates of cobalt and nickel chlorides subjected to a thermal treatment were added to the composites as catalyst precursors. Using thermal analysis and FTIR spectroscopy, it was shown that the amount of water removed increases with the increasing temperature. Herewith, the water molecules that remained in the samples were strongly bound to the metal and isolated from each other. According to the ultraviolet–visible (UV-vis) spectroscopy data, with the increasing temperature of the thermal pretreatment there took place a substitution of a portion of water molecules by chloride ions in the nearest environment of the metal. It appeared that it was the resulting weakening of the electrostatic field on metal that was mainly responsible for the formation of a more finely dispersed catalytic phase of amorphous cobalt boride in the reaction medium under the action of sodium borohydride. The smaller particles of the active components led to a faster rate of gas generation when water was added to the solid-state $NaBH_4$ composites. This trend remained for both the cobalt and the nickel catalytic systems even when the activity was calculated per gram of the metal. Thus, for the preparation of solid-state $NaBH_4$ composites, hydrates of cobalt and nickel chlorides with a low content of water should be used.

**Keywords:** solid-state composite; sodium borohydride; hydrolysis; catalyst; cobalt; nickel

## 1. Introduction

The storage and transportation of hydrogen is a key problem to be solved by the hydrogen economy [1–5]. This problem is especially acute when using low-temperature fuel cells with a proton-exchange membrane (LT-PEMFC) in hard-to-reach and unelectrified areas when hydrogen has to be delivered in a compact form by aircraft transport. In addition to this, hydrogen is to be generated at ambient temperatures from −40 (Antarctica, Alaska, Yakutia, Yamal and other regions of the far north) to +60 °C (deserts, tropics and other regions with hot climate) and with no supply of energy from an outside source. These requirements substantially restrict the range of suitable sources of hydrogen, especially considering the high sensitivity of the LT-PEMFC electrocatalysts towards catalytic poisons, such as CO, $NH_3$, chloride-ions and others [6–8]. The use of composites based on sodium borohydride ($NaBH_4$) containing up to 10 wt % of hydrogen may be an optimum solution to this problem [9,10]. The addition to such composites of a catalyst allows the gas generation to be started immediately after the addition of water.

$$NaBH_4 + 4H_2O \xrightarrow{catalyst} NaB(OH)_4 + 4H_2 \uparrow \quad (1)$$

It should be noted that the catalytic interaction of sodium borohydride with water does not require heating the reaction medium, in contrast to its thermal decomposition, which takes place at temperatures from 130 to 500 °C, even in the presence of active nanosized Ni particles [11], transition metal fluorides [12] and sodium chloride [13].

Hydrogen produced by catalytic $NaBH_4$ hydrolysis contains water vapor as the only impurity [14] and therefore can be supplied to an LT-PEMFC anode space without purification and wetting.

Cheap compounds of cobalt [15–17] or nickel [18–20] are usually added to the solid-state $NaBH_4$ composites. They react with the sodium borohydride to form a catalytically active phase—the amorphous cobalt boride [21]. It was found that in the solid state, during compression, the interaction of sodium borohydride with cobalt chloride already takes place. With the increasing pressures, noticeably greater amounts of salts react with the sodium borohydride, which leads to a faster initial rate of gas generation [22]. It was noted that physicochemical properties such as the dispersion of cobalt catalysts pre-reduced in a solution of sodium borohydride [23] and the crystal structure of a cobalt oxide as catalyst precursor [24] also had an effect on the hydrogen generation rate. However, until now, the effect of physicochemical properties of cobalt and nickel chlorides on the hydrogen generation from solid-state sodium borohydride-based composites has not been studied in detail.

In this work, the kinetics of hydrogen evolution upon the addition of water to solid-state $NaBH_4$ composites with thermally pretreated hydrates of cobalt and nickel chlorides was studied. The physicochemical properties of these catalytic additives were investigated by thermal analysis, Fourier-transform infrared (FTIR) spectroscopy and ultraviolet–visible (UV-vis) spectroscopy. The final aim of this work was to establish the effect of the water content of these metal chlorides on the hydrogen generation rate.

## 2. Results and Discussion

### *2.1. Study of Catalyst Precursors*

Hydrates of cobalt and nickel chlorides thermally pretreated in an inert atmosphere were chosen as the objects of study. It was noted that with the increasing temperature of the heating there was a change in the salts' color. Thus, the untreated cobalt chloride hydrate had a pink color, which changed to violet at 150 °C and became blue at 300 °C. The green nickel chloride hydrate became yellow at 150 °C and at 300 °C its color changed to ocher. With the increasing temperature in an inert atmosphere, there also was an increase in the metal and chlorine contents, indicating that there was a removal of water from the salts (Table 1).

**Table 1.** Characteristics of the catalyst precursors subjected to a thermal treatment for 4 h under argon.

| Temperature of Treatment, °C | Color | Metal Content, wt % | Chlorine Content, wt % | Estimated Water Content, wt % [1] | Empirical Formula of Catalyst Precursor [2] |
|---|---|---|---|---|---|
| **Cobalt chloride hydrate** | | | | | |
| Untreated | Pink | 24.6 | 29.8 | 45.6 | $CoCl_2 \cdot 6.1H_2O$ |
| 150 | Violet | 36.7 | 43.8 | 19.5 | $CoCl_2 \cdot 1.7H_2O$ |
| 300 | Blue | 39.0 | 47.2 | 13.8 | $CoCl_2 \cdot 1.2H_2O$ |
| **Nickel chloride hydrate** | | | | | |
| Untreated | Green | 24.2 | 29.4 | 46.4 | $NiCl_2 \cdot 6.3H_2O$ |
| 150 | Yellow | 33.5 | 39.8 | 26.7 | $NiCl_2 \cdot 2.6H_2O$ |
| 300 | Ocher | 38.1 | 45.2 | 16.7 | $NiCl_2 \cdot 1.4H_2O$ |

[1] Estimated water content = 100 (wt %) − [Metal content (wt %) + Chlorine content (wt %)]. [2] Empirical formulas of salts were used for the designation of catalyst precursors in this article.

According to the results of the thermal analysis, these salts easily lose water beginning from 40 °C (Figure 1a,b). In the temperature region from 40 to 300 °C, four stages of dehydration are distinguishable in the derivative thermogravimetry (DTG) curves. For the cobalt chloride hydrate the greatest losses of mass were observed at 110, 130, 160 and 195 °C. In the case of the nickel chloride hydrate, most of the water was removed at 110 °C, and with further increase in temperature the change in the mass became less pronounced, the lower values being observed in the DTG curves at 185, 215 and 245 °C. It should be noted that at 150 °C almost half of the water was removed from both hydrates. A constant mass of the cobalt and nickel salts was reached at 220 and 280 °C, respectively.

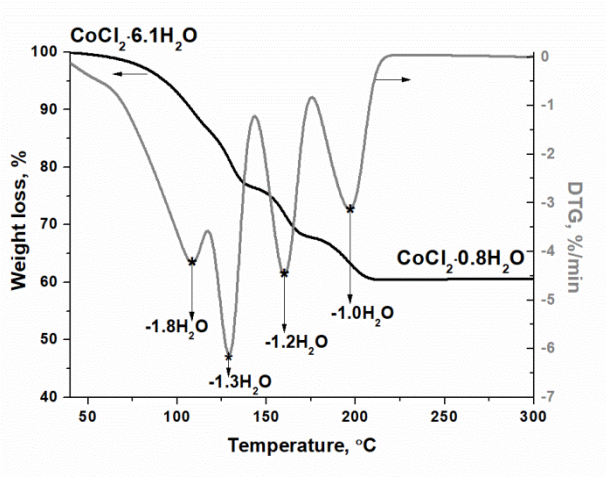


(**a**)

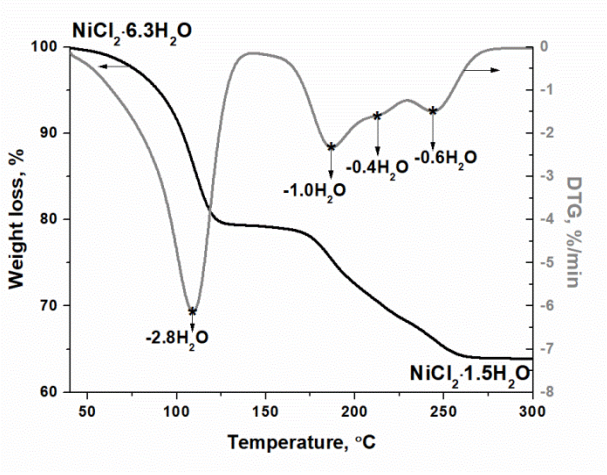


(**b**)

**Figure 1.** Thermal analysis results of water removal from initial salts: (**a**) cobalt chloride hydrate and (**b**) nickel chloride hydrate. Sample mass—100 mg. Feed rate of helium—30 $cm^3$/min. Rate of heating—10 °C/min.

A comparison of the thermal analysis data for untreated hydrates (Figure 1) with the results of the chemical analysis of the samples after their thermal treatment (Table 1) showed that a longer thermal treatment under isothermal conditions led to a content of water in the samples that was lower than the one obtained when they were heated at a rate of 10 °C/min. Nevertheless, the samples treated at 300 °C still contained strongly bound water, which could be removed only at temperatures above 500 °C [25,26].

The presence of water in hydrates of cobalt and nickel chlorides follows from the results of the FTIR spectroscopy. The FTIR spectrum of the untreated salts $NiCl_2 \cdot 6.3H_2O$ and $CoCl_2 \cdot 6.1H_2O$ (Figure 2) shows absorption bands corresponding to the vibrations of water [27,28].

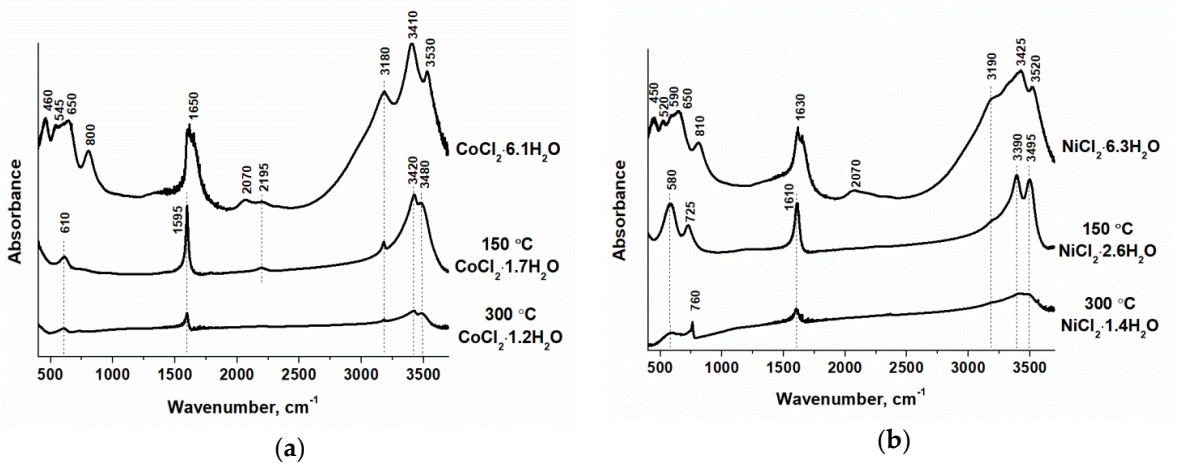


**Figure 2.** FTIR spectra of (**a**) cobalt chloride hydrate, (**b**) nickel chloride hydrate and their partially dehydrated species obtained under isothermal condition.

The low-frequency region of the FTIR spectrum shows librational vibrations (fan-shaped, torsional and pendular) of water molecules coordinated by cobalt ions. The broad absorption bands (a.b.) with the center of gravity at 1630 $cm^{-1}$ for the salt of nickel and at 1650 $cm^{-1}$ for the cobalt salt belong to the deformational scissor vibrations of water, with the overtone at 3100–3250 $cm^{-1}$, which gives a well-pronounced shoulder of the a.b. at 3185 ± 5 $cm^{-1}$. The presence of a.b. at 2070 and 2195 $cm^{-1}$ indicates that there is a sum of librational and deformational vibrations of water molecules. The intense absorption in the high-frequency region with clearly pronounced maxima at 3190 and 3425 $cm^{-1}$ for the nickel salts and at 3180 and 3410 $cm^{-1}$ for the cobalt salts is a superposition of symmetrical and asymmetrical valence vibrations of water. The a.b. at 3525 ± 5 $cm^{-1}$ is indicative of the presence in the metal hydrates of weakly bound water molecules whose valence vibrations show themselves in the region of 3500–3600 $cm^{-1}$.

The thermal treatment of nickel and cobalt chloride hydrates led to a noticeable decrease in the intensity of the FTIR spectra because of the water removal. The intense absorption at 1600–1700 $cm^{-1}$ turned into a sharp symmetrical a.b. with the maximum shifted towards lower frequencies, indicating that the water molecules were isolated from each other [29]. Moreover, the number of a.b. in the region of 400–800 $cm^{-1}$ due to the librational vibrations was reduced because of the reduced vibrational degrees of freedom of the water molecule as a result of a stronger bonding between metal and water molecules in the thermally treated samples.

The dehydration of cobalt and nickel chloride hydrates leads, first of all, to changes in the nearest environment of the metal. According to the UV-vis data, in the untreated salts water was directly coordinated to the metal, since their UV-vis spectra showed a.b. which, according to [30], are assignable to d-d-transitions in the six-coordinated aquacomplexes $[Ni(H_2O)_6]^{2+}$ and $[Co(H_2O)_6]^{2+}$ (Figure 3). For the cobalt chloride hydrate, the most intense absorption was observed in the region of 250–500 nm with a maximum at 430 nm ($4T_{1g}(F) \rightarrow 4T_{2g}(P)$). The multiple structure of this a.b. is a result of admixture to the mainly 2G and 2H associated doublet state of spin-forbidden d-d transitions. The second d-d transition $4T_{1g}(F) \rightarrow 4A_{2g}$ was very weak and appeared as a shoulder at 560 nm.

Characteristic of the six-coordinated nickel aqua-complex $[Ni(H_2O)_6]^{2+}$ are spin-allowed d-d transitions: 300 nm ($3A_{2g} \rightarrow 3T_{1g}(P)$) and 655 nm ($3A_{2g} \rightarrow 3T_{1g}$). In addition to this, two spin-forbidden d-d transitions were well noticeable against their background: 590 nm ($3A_{2g} \rightarrow 1E_g(D)$) and 365 nm ($3A_{2g} \rightarrow 1T_{2g}(D)$).

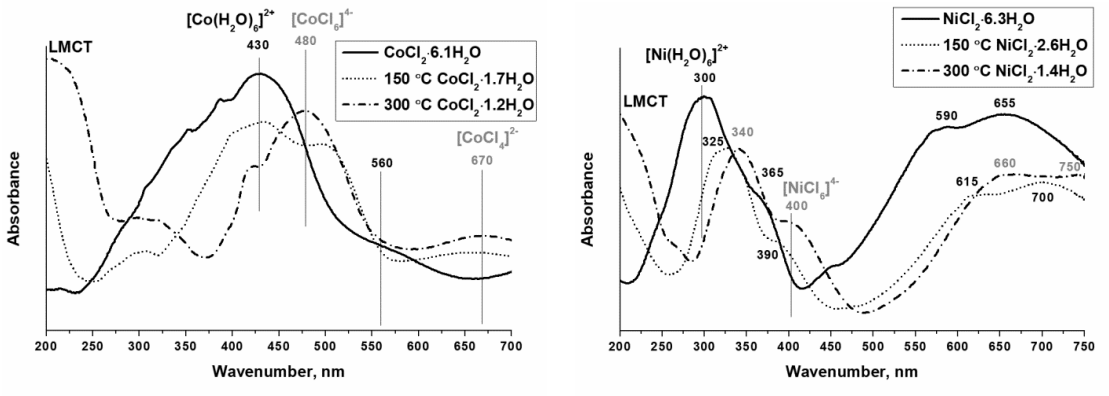


(**a**) (**b**)

**Figure 3.** UV-vis spectra of (**a**) cobalt chloride hydrate and (**b**) nickel chloride hydrate, as well as of their partially dehydrated species.

After thermal treatment, the a.b. corresponding to the d-d transitions were shifted towards lower frequencies, which is indicative of a weakening of the ligand field as a result of the replacement of water by chloride ions in the nearest environment of the metal [31]. In the spectrochemical series, the chloride ion position is to the left of that of the water [32]:

$I^- < Br^- < S^{2-} < Cl^- < SCN^- < NO_3^- < N_3^- < F^- < OH^- < C_2O_4^{2-} < H_2O < NCS^- < CH_3CN <$ pyridine $< NH_3 <$ ethylenediamine $<$ 2,2′-bipyridine $< NO_2^- < PPh_3 < CN^- < CO$

Besides, characteristic of a partially dehydrated cobalt is the appearance of a weak a.b. at 670 nm (Figure 3a), which corresponds to the d-d-transition $^4A_2 \rightarrow {}^4T_1$ [33,34] in the four-coordinated tetrahedral complex $[CoCl_4]^{2-}$.

Apart from the changes relating to the d-d transitions, there also was a large low-frequency shift of the ligand-to-metal charge-transfer (LMCT) band and an increase in its intensity. According to [35], these changes were caused by the removal of water from the nearest environment of the metal. Hence, in the thermally treated samples of the hydrates, water in the first coordination sphere of the metal was partially replaced by chloride ions which had a weaker electrostatic field. In the case of the cobalt salt, there also was a change in the symmetry of the local environment of the central metal ion. The water molecules that remained in the samples were strongly bound to the metal and isolated from each other.

### *2.2. Study of Catalytic Sodium Borohydride Hydrolysis*

Hydrates of cobalt and nickel chlorides treated at different temperatures were used to prepare solid-state hydrogen-generating composites based on sodium borohydride (Figure 4). The hydrogen content in the tablet of composite was not less than 8.4 wt % (Table 2).

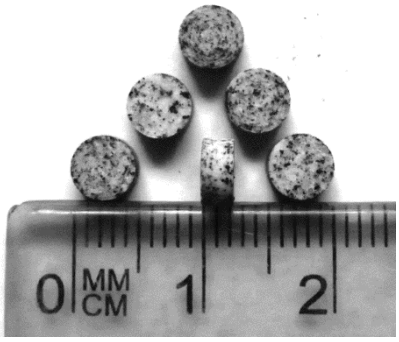


**Figure 4.** Solid-state hydrogen-generating composite based on sodium borohydride.

**Table 2.** Kinetics parameters of hydrogen generation during sodium borohydride hydrolysis over cobalt and nickel catalysts.

| Empirical Formula of Catalyst Precursor | Tablet Mass, g | Metal Mass, g | Hydrogen Content, wt % | Catalytic Activity, $cm^3_{H2}/s \cdot g_M$ |
|---|---|---|---|---|
| **Cobalt catalysts** | | | | |
| $CoCl_2 \cdot 6.1H_2O$ | 0.0495 | 0.0024 | 8.45 | 118 |
| $CoCl_2 \cdot 1.7H_2O$ | 0.0525 | 0.0039 | 8.40 | 135 |
| $CoCl_2 \cdot 1.2H_2O$ | 0.0573 | 0.0045 | 8.40 | 152 |
| **Nickel catalysts** | | | | |
| $NiCl_2 \cdot 6.3H_2O$ | 0.0502 | 0.0024 | 8.45 | 23 |
| $NiCl_2 \cdot 2.6H_2O$ | 0.0551 | 0.0037 | 8.41 | 27 |
| $NiCl_2 \cdot 1.4H_2O$ | 0.0537 | 0.0041 | 8.41 | 34 |

The catalytically active phase in the form of amorphous cobalt and nickel borides was observed to form already during the preparation of the tablets, as a result of a solid-state interaction between the hydride and the metal salts [22]. Therefore, hydrogen generation started immediately after the addition of water to the solid composite, which dissolved instantaneously. Figure 5 shows hydrogen generation as a function of the water content in the cobalt and nickel chloride hydrates.

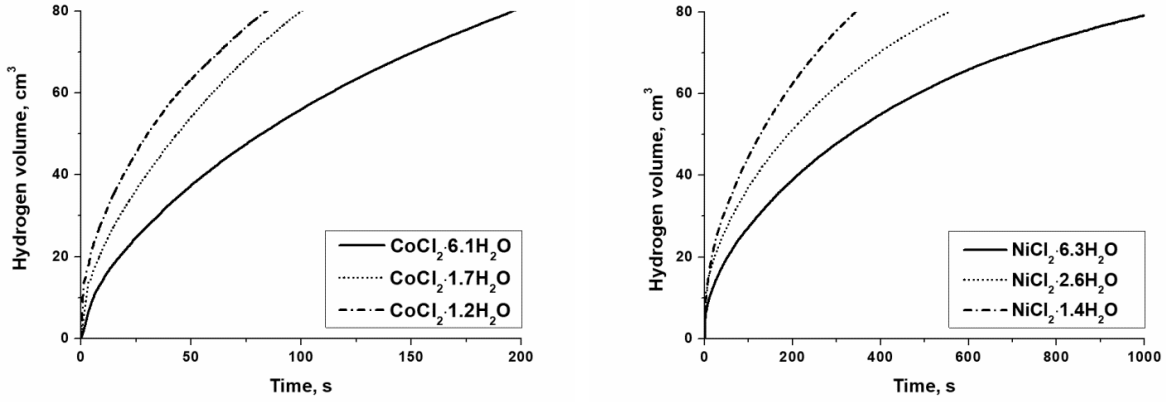


(**a**) (**b**)

**Figure 5.** Effect of water content in (**a**) cobalt and (**b**) nickel chloride hydrates on the hydrogen generation from solid-state $NaBH_4$ compositions.

According to our study, the smaller the water content in the salts, the higher the hydrogen generation rate. This trend remained both for the cobalt and nickel catalytic systems even when their activity was calculated per gram of the metal (Table 2).

It should be noted that the by-product of sodium borohydride hydrolysis is $NaB(OH)_4$ [36].

### *2.3. Study of Catalysts after Reaction*

To establish the reasons for such dependence, the cobalt and nickel catalysts were separated from the reaction medium and studied by transmission electron microscopy (TEM). It was found that particles of the catalyst active component formed under the action of sodium borohydride were amorphous (Figures 6 and 7) and contained both the metal (Co or Ni) and the boron (Table 3). The particle surface was coated with an oxygen-containing shell up to 5 nm thick [21]. The average sizes of the particles forming from the initial cobalt and nickel salts were 16.7 and 7.2 nm, respectively. The analysis of the particle size distribution (Figures 6d and 7d) showed that the dehydration of salts resulted in the formation of smaller particles of the catalyst. From Table 3 it is seen that with the loss

of water there was a decrease in the average diameter of the cobalt catalysts from 16.7 to 13.2 nm. The average particle size of the nickel catalysts also decreased from 7.2 to 5.5 nm.

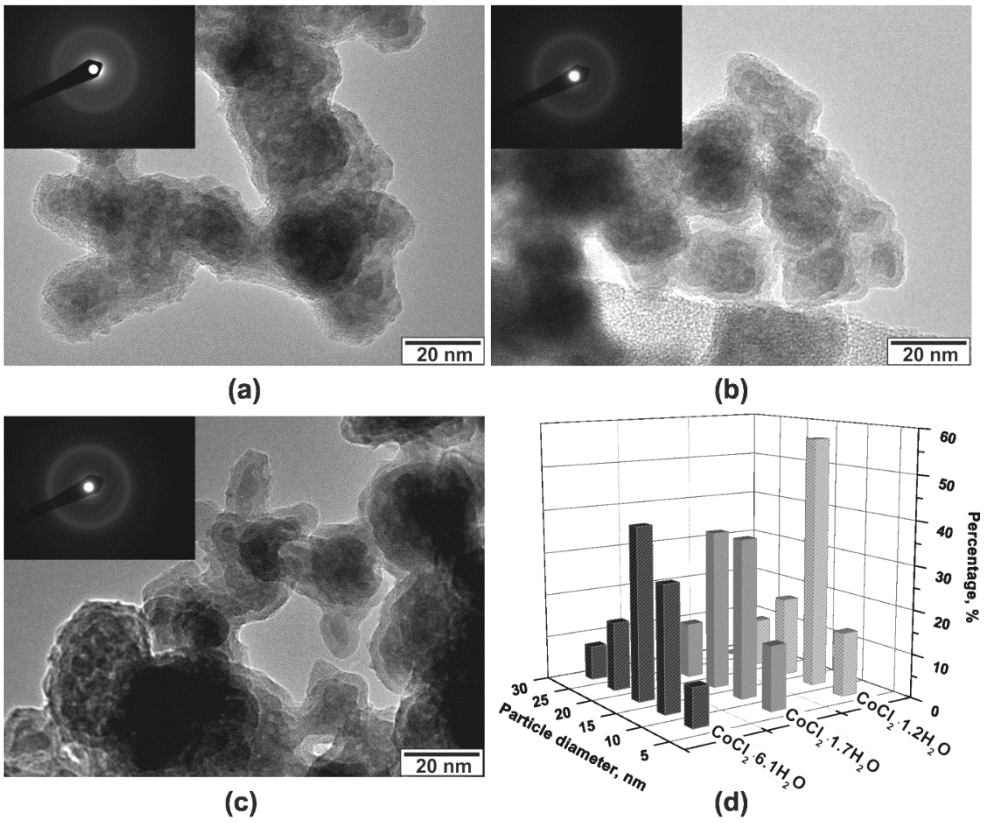


**Figure 6.** TEM images of cobalt catalysts forming from (**a**) $CoCl_2 \cdot 6.1H_2O$, (**b**) $CoCl_2 \cdot 1.7H_2O$ and (**c**) $CoCl_2 \cdot 1.2H_2O$, and (**d**) their particle size distribution.

**Table 3.** Characteristics of reduced catalysts after sodium borohydride hydrolysis.

| Empirical Formula of Catalyst Precursor | Phase | Average Particle Size [1], nm | Content, wt % | | |
|---|---|---|---|---|---|
| | | | Co | Ni | B |
| **Cobalt catalysts** | | | | | |
| $CoCl_2 \cdot 6.1H_2O$ | amorphous | 16.7 | 64.3 | - | 4.1 |
| $CoCl_2 \cdot 1.7H_2O$ | | 14.9 | 63.2 | - | 4.5 |
| $CoCl_2 \cdot 1.2H_2O$ | | 13.2 | 61.6 | - | 4.5 |
| **Nickel catalysts** | | | | | |
| $NiCl_2 \cdot 6.3H_2O$ | amorphous | 7.2 | - | 73.9 | 4.6 |
| $NiCl_2 \cdot 2.6H_2O$ | | 6.3 | - | 72.5 | 5.1 |
| $NiCl_2 \cdot 1.4H_2O$ | | 5.5 | - | 72.6 | 5.2 |

[1] as surface area-weighted diameter (Equation (4)).

Thus, the higher activity of the dehydrated salts in the sodium borohydride hydrolysis resulted from a change in the size of the catalyst particles forming in the reaction medium under the action of hydride. A possible reason for such a behavior may be the weakening of the ligand field due to a partial substitution of water by chloride ions in the nearest environment of the metal, which led to a faster formation of the small particles of amorphous metal borides catalyzing the interaction between the hydride and water.

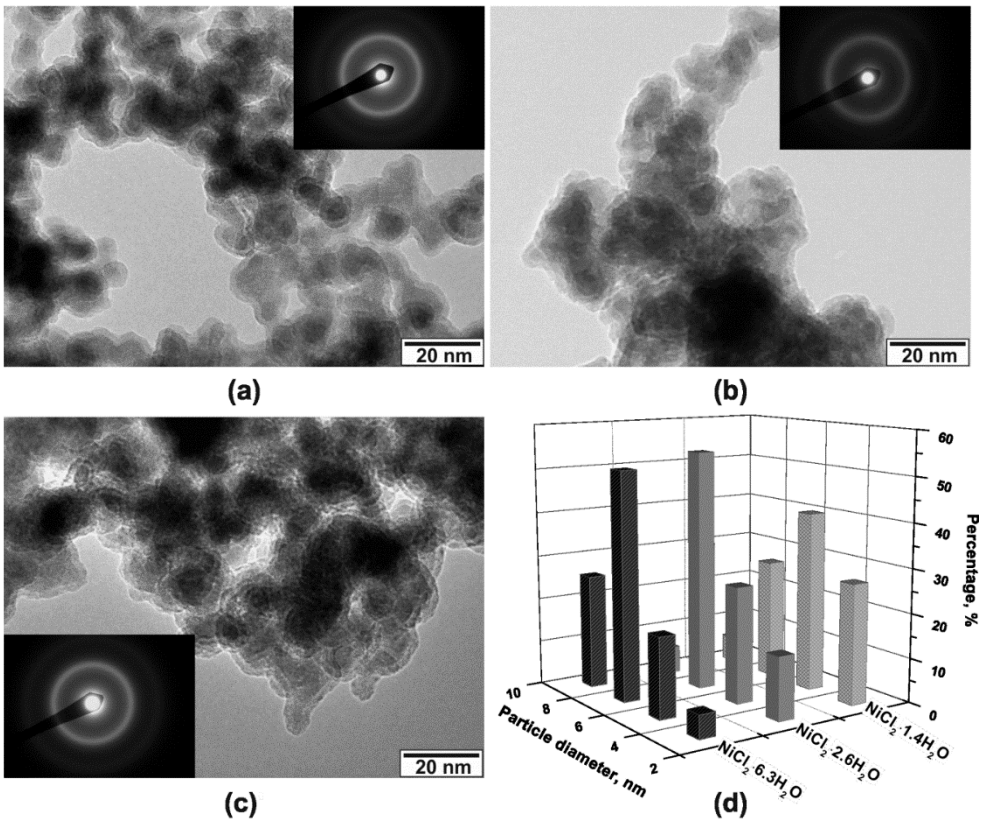


**Figure 7.** TEM images of nickel catalysts forming from (**a**) $NiCl_2 \cdot 6.3H_2O$, (**b**) $NiCl_2 \cdot 2.6H_2O$ and (**c**) $NiCl_2 \cdot 1.4H_2O$, and (**d**) their particle size distribution.

## 3. Materials and Methods

Solid-state hydrogen-generating composites were prepared from a mechanical mixture of sodium borohydride (CAS 16940-66-2; Sigma-Aldrich 452882) and catalyst precursor.

Cobalt chloride hydrate (CAS 7791-13-1; Sigma-Aldrich 255599) and nickel chloride hydrate (CAS 69098-15-3; Sigma-Aldrich 364304) were used as catalyst precursors. Their dehydrated species were prepared by thermal treatment at 150 and 300 °C in a 30 $cm^3$/min flow of argon with subsequent storage in a desiccator under argon to prevent water absorption.

Samples of the reagents were ground in a mortar grinder (PULVERISETTE 2, FRITSCH GmbH, Industriestrasse 8, 55743 Idar-Oberstein Germany) during 2 min and compressed into tablets using a manual tablet press machine (TDP-0, SINOPED, No. 85, Ganqu Road, Taizihe District, Liaoyang, Liaoning, China) at an air humidity of 30 %. The compression was performed at 27 kgf/$cm^2$, since this pressure was shown [22], on the one hand, to ensure a rapid dissolution of the tablet in water, and on the other to initiate the formation of the catalytically active component by a solid-state interaction of the hydride with the salts (Table 4):

$$4\{MCl_2 \cdot 6H_2O\} + 8NaBH_4 \rightarrow \left\{4M^0 + 2B^0\right\}_{catalyst} + 6B(OH)_3 + 8NaCl + 6H_2O + 25\,H_2 \uparrow \quad (2)$$

**Table 4.** Half-reactions of cobalt and nickel chlorides reduction by sodium borohydride.

| Reduction Half-reactions: | Oxidation Half-Reactions: |
|---|---|
| $4M^{2+} + 8e^- \rightarrow 4M^0$ | $2BH_4^- - 2e^- \rightarrow 2B^0 + 4H_2 \uparrow$ |
| $18H_2O + 18e^- \rightarrow 18OH^- + 9H_2 \uparrow$ | $6BH_4^- - 24e^- \rightarrow 6B^{3+} + 12H_2 \uparrow$ |

The metal and chlorine contents of the catalyst precursors were determined by X-ray fluorescence analysis on a VRA-30 instrument with a Cr anode of the X-ray tube. The relative error of determination was ±5%. Using the data of the elemental analysis, the water content in the hydrates of cobalt and nickel chlorides was calculated:

$$Water\,content\,(wt\ \%) = 100 - (Metal\,content\,(wt\ \%) + Chlorine\,content\,(wt\ \%)) \quad (3)$$

The empirical formulas of the salts were calculated as the ratio of moles of salt ($CoCl_2$ or $NiCl_2$) to water ($H_2O$). The empirical formulas of the salts were used for the designation of catalyst precursors in this article.

The metal and boron contents of the reduced catalyst were determined by inductively coupled plasma atomic emission spectroscopy on an Optima 4300 DV instrument (PerkinElmer Inc., 45 William Street, Wellesley, MA 02481-4078, USA). For the determination of elements, the samples were dissolved by using hydrochloric acid. The relative error of determination was ±5%.

The catalyst precursors were studied by Thermal Analysis (TA), Fourier-Transform Infrared spectroscopy (FTIR) and Ultraviolet–Visible spectroscopy (UV-vis).

The thermal analysis was carried out on a Netzsch STA 449 C Jupiter (NETZSCH-Gerätebau GmbH, Wittelsbacherstraße 42, 95100 Selb, Germany) instrument equipped with a DTA/TG holder in the temperature range of 40–300 °C in a flow of He (30 $cm^3$/min). The heating rate of the samples (100 mg) was 10 °C/min.

The FTIR spectra were taken at room temperature on a FTIR Varian 640-IR (Agilent Technologies, 5301 Stevens Creek Blvd, Santa Clara, CA 95051, USA) spectrometer. Prior to the spectral measurements, the 5 mg samples were mixed with 400 mg of KBr and compressed into tablets.

The UV-vis diffuse reflectance spectra were recorded at room temperature in the range of 200–700 nm with a resolution of 1 nm using a Cary 100 UV–Vis Varian (Agilent, 5301 Stevens Creek Blvd., Santa Clara, CA 95051, USA) spectrometer equipped with a DRA-30I diffuse reflectance accessory.

The reduced catalysts were studied by transmission electron microscopy (TEM). They were separated from the reaction medium with a magnet, washed three times with distilled water and three times with acetone. The catalysts were then evacuated at room temperature for 24 h, after which they were stored in a desiccator under an inert medium (argon) to prevent sample oxidation by air oxygen. Electron microscopy images of the catalysts were obtained on a JEM-2010 electron microscope with an accelerating voltage of 200 kV and a resolving power of 1.4 Å. The samples to be analyzed were applied to a holey carbon film fixed on a standard copper grid. Size distribution diagrams were constructed using measured diameters ($d_i$) of at least 300 particles ($n_i$). The mean particle sizes were quoted [37] as a surface area-weighted diameter ($\overline{d_s}$):

$$\overline{d_s} = \sum_i n_i d_i^3 / \sum_i n_i d_i^2 \quad (4)$$

The kinetics of sodium borohydride hydrolysis was studied in a temperature controlled glass reactor at 40 °C. The solid-state $NaBH_4$ composite was placed into the reactor and then 10 mL of deionized water was added. The volume of the evolved hydrogen was measured using a 100 mL gas burette with a resolution of 0.2 mL. The data obtained were corrected to Standard Temperature and Pressure – S.T.P. - (0 °C, 1 atm) based on three repeated experiments carried out under the same conditions. The experimental uncertainty was less than 2%.

The catalytic activity (A) was determined as the average rate ($\overline{r}$) of hydrogen evolution ($cm^3$/s) referred to the mass ($m_M$) of the metal (g) in the $NaBH_4$ composite:

$$A = \frac{\overline{r}}{m_M} \quad (5)$$

## 4. Conclusions

Hydrates of cobalt and nickel chlorides after thermal treatment at 150 and 300 °C were used as catalytic precursors for solid-state hydrogen-generation composites based on sodium borohydride. Using thermal analysis and FTIR spectroscopy, it was found that thermal treatment led to the removal of water from the salts, which increased with the increasing temperature. According to the UV-vis data, in the first coordination sphere of a metal (cobalt or nickel), water molecules were partially replaced by chloride ions, which have a weaker electrostatic field. Apparently, the weakening of the ligand field led to the formation of smaller particles of the active catalytic phase of amorphous metal borides. Thus, the higher activity of the dehydrated salts in the sodium borohydride hydrolysis is a result of the smaller size of the catalyst particles forming in the reaction medium under the action of sodium borohydride.

Summarizing the results of our study, it may be concluded that the hydrates of cobalt and nickel chlorides used for the preparation of solid-state $NaBH_4$ composites should preferably have a low content of water.

**Author Contributions:** This study was conducted with contributions from all authors. Conceptualization, V.I.S.; methodology and formal analysis, A.A.P.; investigation, O.V.K. and O.V.N., writing and original draft preparation, O.V.N.; writing, review and editing, O.V.N.; visualization, O.V.K., supervision, V.I.S. All authors have read and agreed to the published version of the manuscript.

**Funding:** This work was supported by the Ministry of Science and Higher Education of the Russian Federation (project AAAA-A17-117041710089-7).

**Acknowledgments:** The authors are grateful to Nikolaeva O.A. and Ishchenko A.V. for their technical support.

**Conflicts of Interest:** The authors declare no conflict of interest. The funders had no role in the design of the study; in the collection, analyses or interpretation of data; in the writing of the manuscript; or in the decision to publish the results.

## References

1. Sinigaglia, T.; Lewiski, F.; Santos Martins, M.E.; Mairesse Siluk, J.C. Production, storage, fuel stations of hydrogen and its utilization in automotive applications—A review. *Int. J. Hydrogen Energy* **2017**, *42*, 24597–24611. [CrossRef]
2. Abe, J.O.; Popoola, A.P.I.; Ajenifuja, E.; Popoola, O.M. Hydrogen energy, economy and storage: Review and recommendation. *Int. J. Hydrogen Energy* **2019**, *44*, 15072–15086. [CrossRef]
3. Rivard, E.; Trudeau, M.; Zaghib, K. Hydrogen storage for mobility: A review. *Materials* **2019**, *12*, 1973. [CrossRef]
4. Moradi, R.; Groth, K.M. Hydrogen storage and delivery: Review of the state of the art technologies and risk and reliability analysis. *Int. J. Hydrogen Energy* **2019**, *44*, 12254–12269. [CrossRef]
5. Staffel, I.; Scamman, D.; Velazquez Abad, A.; Balcombe, P.; Dodds, P.E.; Ekins, P.; Shah, N.; Ward, K.R. The role of hydrogen and fuel cells in the global energy system. *Energy Environ. Sci.* **2019**, *12*, 463–491. [CrossRef]
6. Oetjen, H.-F.; Schmidt, V.M.; Stimming, U.; Trila, F. Performance data of a proton exchange membrane fuel cell using $H_2$/CO as fuel gas. *J. Electrochem. Soc.* **1996**, *143*, 3838–3842. [CrossRef]
7. Hongrapipat, J.; Saw, W.L.; Pang, S. Removal of ammonia from producer gas in biomass gasification: Integration of gasification optimisation and hot catalytic gas cleaning. *Biomass Conv. Biorefin.* **2012**, *2*, 327–348. [CrossRef]
8. Job, N.; Chatenet, M.; Berthon-Fabry, S.; Hermans, S.; Maillard, F. Efficient Pt/carbon electrocatalysts for proton exchange membrane fuel cells: Avoid chloride-based Pt salts! *J. Power Sour.* **2013**, *240*, 294–305. [CrossRef]
9. Hsueh, C.-L.; Liu, C.-H.; Chen, B.-H.; Lee, M.-S.; Chen, C.-Y.; Lu, Y.-W.; Tsau, F.; Ku, J.-R. A novel design of solid-state $NaBH_4$ composite as a hydrogen source for 2 W PEMFC applications. *J. Power Sour.* **2011**, *196*, 3530–3538. [CrossRef]
10. Boran, A.; Erkan, S.; Eroglu, I. Hydrogen generation from solid state $NaBH_4$ by using $FeCl_3$ catalyst for portable proton exchange membrane fuel cell applications. *Int. J. Hydrogen Energy* **2019**, *44*, 18915–18926. [CrossRef]

11. Liu, Y.; Heere, M.; Contreras Vasquez, L.; Paterakis, C.; Sørby, M.H.; Hauback, B.C.; Book, D. Dehydrogenation and rehydrogenation of a 0.62$LiBH_4$-0.38$NaBH_4$ mixture with nano-sized Ni. *Int. J. Hydrogen Energy* **2018**, *43*, 16782–16792. [CrossRef]
12. Kalantzopoulos, G.N.; Guzik, M.N.; Deledda, S.; Heyn, R.H.; Muller, J.; Hauback, B.C. Destabilization effect of transition metal fluorides on sodium borohydride. *Phys. Chem. Chem. Phys.* **2014**, *16*, 20483–20491. [CrossRef]
13. Olsen, J.E.; Sørby, M.H.; Hauback, B.C. Chloride-substitution in sodium borohydride. *J. Alloys Compd.* **2011**, *509*, L228–L231. [CrossRef]
14. Netskina, O.V.; Filippov, T.N.; Komova, O.V.; Simagina, V.I. Hydrogen generation by acidic and catalytic hydrolysis of sodium borohydride. *Catal. Sustain. Energy* **2018**, *5*, 41–48. [CrossRef]
15. Kim, T. Hydrogen production from solid sodium borohydride with hydrogen peroxide decomposition reaction. *Int. J. Hydrogen Energy* **2010**, *35*, 12870–12877. [CrossRef]
16. Liu, C.-H.; Kuo, Y.-C.; Chen, B.-H.; Hsueh, C.-L.; Hwang, K.-J.; Ku, J.-R.; Tsau, F.; Jeng, M.-S. Synthesis of solid-state $NaBH_4$/Co-based catalyst composite for hydrogen storage through a high-energy ball-milling. *Int. J. Hydrogen Energy* **2010**, *35*, 4027–4040. [CrossRef]
17. Netskina, O.V.; Komova, O.V.; Simagina, V.I. Developing effective cobalt catalysts for hydrogen-generating solid-state $NaBH_4$ composite. *Catal. Ind.* **2018**, *10*, 166–172. [CrossRef]
18. Prosini, P.P.; Gislon, P. Water consumption during solid state sodium borohydride hydrolysis. *Int. J. Hydrogen Energy* **2010**, *35*, 12234–12238. [CrossRef]
19. Demirci, U.B. Sodium borohydride for the near-future energy: A «Rough Diamond» for Turkey. *Turk. J. Chem.* **2018**, *42*, 193–220. [CrossRef]
20. Lai, Q.; Alligier, D.; Aguey-Zinsou, K.-F.; Demirci, U.B. Hydrogen generation from a sodium borohydride–nickel core@shell structure under hydrolytic conditions. *Nanoscale Adv.* **2019**, *1*, 2707–2717. [CrossRef]
21. Netskina, O.V.; Kochubey, D.I.; Prosvirin, I.P.; Malykhin, S.E.; Komova, O.V.; Kanazhevskiy, V.V.; Chukalkin, Y.G.; Bobrovskii, V.I.; Kellerman, D.G.; Ishchenko, A.V.; et al. Cobalt-boron catalyst for $NaBH_4$ hydrolysis: The state of the active component forming from cobalt chloride in a reaction medium. *Mol. Catal.* **2017**, *441*, 100–108. [CrossRef]
22. Netskina, O.V.; Tayban, E.S.; Ozerova, A.M.; Komova, O.V.; Simagina, V.I. Solid-state $NaBH_4$/Co composite as hydrogen storage material: Effect of the pressing pressure on hydrogen generation rate. *Energies* **2019**, *12*, 1184. [CrossRef]
23. Netskina, O.V.; Ozerova, A.M.; Komova, O.V.; Odegova, G.V.; Simagina, V.I. Hydrogen storage systems based on solid-state $NaBH_4/Co_xB$ composite: Influence of catalyst properties on hydrogen generation rate. *Catal. Today* **2015**, *245*, 86–92. [CrossRef]
24. Simagina, V.I.; Ozerova, A.M.; Komova, O.V.; Odegova, G.V.; Kellerman, D.G.; Fursenko, R.V.; Odintsov, E.S.; Netskina, O.V. Cobalt boride catalysts for small-scale energy application. *Catal. Today* **2015**, *242*, 221–229. [CrossRef]
25. Mishra, S.K.; Kanungo, S.B. Thermal dehydration and decomposition of nickel chloride hydrate ($NiCl_2xH_2O$). *J. Therm. Anal.* **1992**, *38*, 2417–2436. [CrossRef]
26. Mishra, S.K.; Kanungo, S.B. Thermal dehydration and decomposition of cobalt chloride hydrate ($CoCl_2xH_2O$). *J. Therm. Anal.* **1992**, *38*, 2437–2454. [CrossRef]
27. Gamo, I. Infrared spectra of water of crystallization in some inorganic chlorides and Sulfates. *Bull. Chem. Soc. Jpn.* **1961**, *34*, 760–764. [CrossRef]
28. Brubach, J.B.; Mermet, A.; Filabozzi, A.; Gerschel, A.; Roy, P. Signatures of the hydrogen bonding in the infrared bands of water. *J. Chem. Phys.* **2005**, *122*, 184509. [CrossRef]
29. Vasylieva, A.; Doroshenko, I.; Doroshenko, O.; Pogorelov, V. Effect of argon environment on small water clusters in matrix isolation. *Low Temp. Phys.* **2019**, *45*, 627. [CrossRef]
30. Carlin, R.L. *Inorganic Electronic Spectroscopy (Lever, A.B.P.)*; ACS Publications: Washington, DC, USA, 1984.
31. Howell, O.R.; Jackson, A. The change in the absorption spectrum of cobalt chloride in aqueous solution with increasing concentration of hydrochloric acid. *Proc. R. Soc. A Math. Phys.* **1933**, *142*, 587–597. [CrossRef]
32. Huheey, J.E.; Keiter, E.A.; Keiter, R.L. *Inorganic Chemistry: Principles of Structure and Reactivity*; Harper-Collins: New York, NY, USA, 1993.

33. Pan, P.; Susak, N.J. Co(II)-chloride and bromide complexes in aqueous solutions up to 5 m NaX and 90 °C: Spectrophotometric study and geological implications. *Geochim. Cosmochim. Acta* **1989**, *53*, 327–341. [CrossRef]
34. Uchikoshi, M. Determination of the distribution of cobalt-chloro complexes in hydrochloric acid solutions at 298 K *J. Solut. Chem.* **2018**, *47*, 2021–2038. [CrossRef]
35. De vries, C.G. A Study of the Vogel Reaction for the Determination of Cobalt. Master's Thesis, Louisiana State University, Baton Rouge, LA, USA, 1949. Available online: https://digitalcommons.lsu.edu/gradschool_disstheses/7927 (accessed on 15 October 2019).
36. Netskina, O.V.; Komova, O.V.; Simagina, V.I.; Odegova, G.V.; Prosvirin, I.P.; Bulavchenko, O.A. Aqueous-alkaline $NaBH_4$ solution: The influence of storage duration of solutions on reduction and activity of cobalt catalysts. *Renew. Energy* **2016**, *99*, 1073–1081. [CrossRef]
37. Netskina, O.V.; Kochubey, D.I.; Prosvirin, I.P.; Kellerman, D.G.; Simagina, V.I.; Komova, O.V. Role of the electronic state of rhodium in sodium borohydride hydrolysis. *J. Mol. Catal. A Chem.* **2014**, *390*, 125–132. [CrossRef]